AN ABSTRACT OF THE THESIS OF

Yongsheng Liu for the degree of Master of Science in Mechanical Engineering presented on November 6, 1992.

Title: An Analysis of Peripheral Milling of Finger-joints in Ponderosa Pine Cut-Stock

Redacted for Privacy

Abstract approved: _____
Clarence A. Calder

To make low grade lumber into high-valued products, finger-jointing is a widely used method in the timber industry. In certain situations, chip-out occurs degrading the quality of the joint. To better understand the machining process, a beam-type dynamometer based on strain gages was designed to analyze the dynamic cutting forces parallel and vertical to the feeding direction. The test results indicate that the dynamometer design was sensitive enough to measure small force changes at relatively high frequencies during the cutting operation.

The test conditions were set as close as possible to that in industry. Cutting force behavior of the rotating cutterhead was examined, and test samples with different fiber angles were used for inspecting the influences on the chip-out occurrence and cutting forces. The results show that cutting forces are determined by the density of the wood and the maximum chip thickness. Slight differences in tool shape and the balance of the cutterhead can vary the cutting force behavior. The occurrence of chip-out is dependent on the fiber angle and the chip thickness. No relationship between chip-out and cutting

force was found, within the sensitivity of the dynamometer. Fiber angle has some effect on the cutting force, and also influences the cutting surface quality.

A high speed video camera was also employed to visually observe the formation of chip-out. Frame by frame analysis showed that the chip-out occured when a knife passed through the trailing edge of the cut-block, and the failure developed in the sequel cuts.

Cutting force and chip-out models were developed from the experiment results, and can be used to reduce chip-out and increase recovery during finger-jointing in ponderosa pine cut-stock operation.

An Analysis of Peripheral Milling of Finger-joints in Ponderosa Pine Cut-Stock

by

Yongsheng Liu

A THESIS

submitted to

Oregon State University

in partial fulfillment of
the requirements for the
degree of

Master of Science

Completed November 6, 1992

Commencement June 1993

APPROVED:

Redacted for Privacy

Associate Professor of Mechanical Engineering in charge of major

Redacted for Privacy

Head of department of Mechanical Engineering

Redacted for Privacy

Dean of Graduate School

Date thesis is presented November 6, 1992

Typed by Yongsheng Liu for Yongsheng Liu

ACKNOWLEDGEMENT

First of all, I would like to express my deepest gratitude to my major professor, Dr. Clarence A. Calder, whose continuous guidance and support during my graduate studies has been invaluable.

I would like to extend my earnest thanks to Professor Charles C. Brunner, III and Professor James W. Funck in the Department of Forest Products, for giving me the chance to complete this project. Without their inestimable advice and support, the fulfillment of this thesis would have been impossible.

My sincere thanks is also extended to Professor Gordon M. Reistad, head of the Department of Mechanical Engineering, for providing me financial assistance to support my graduate studies. A special thanks also goes to Mr. Orrie Page, mechanical technician, for his kind help with machining required. Appreciation is also extended to many professors and fellow students who gave me valuable advice and help.

My heartfelt thanks goes to my parents, Yanzhi Lu and Zeng Liu, for their constant encouragement and love, which has motivated my enthusiasm during all my studies. Finally, I would like to thank my wife, Xuan Cheng, for her devoted support which made this endeavor a reality.

This project was funded by a special grant from the US Department of Agriculture and the McItire Stennis Program.

TABLE OF CONTENTS

LIST OF FIGURES

LIST OF TABLES

AN ANALYSIS OF PERIPHERAL MILLING OF FINGER-JOINTS IN PONDEROSA PINE CUT-STOCK

I. INTRODUCTION

The machining of finger-joints in the timber industry using a rotating cutterhead is a precise peripheral milling operation. Considerable economic and recovery gains can be made if the crosscut line can be placed closer to a defect, such as a knot. However, a cut too close to a knot may cause chipping from the edge of the cutting block, known as chip-out, which degrades the quality of the joint.

A previous study by Coombs (1988) examined translational cutting forces and factors controlling the occurrence of chip-out. His research used very slow orthogonal cutting to estimate the cutting forces generated in peripheral milling of finger-joints. However, the estimation may not be accurate due to rate effects resulting from the dynamic cutting force of the rotating cutterhead.

The objective of this project was to refine Coombs' chip-out and cutting force models by using peripheral cutting on a milling machine. A beam type dynamometer using semi-conductor strain gages was designed to ensure sufficient sensitivity of force measurement. A moderate speed digital data acquisition system was employed for dynamic force measurement. The formation of chip-out was visually observed frame by frame using a high speed video system.

Presentation of the results of this study are organized in four sections. First, basic knowledge of wood cutting and previous studies in this area are discussed in the section titled "Literature Review". The design of the dynamometer and test procedures are described next in "Methods and Materials". Test results including tables and figures are given in "Results and Discussions" along with discussion of results and comparison with previous studies. The final section contains conclusions of the study.

II. LITERATURE REVIEW

1. Terminology

There is no strict standard for the terminology used in wood cutting geometry. The main terms and definitions used in this thesis are described below and are based on terminology used in previous studies (see Franz, 1958; Coombs, 1988). The basic geometrical relationships are shown in Figure 1 and defined as follows:

Cutting angle, α — the angle between the tool face and a plane perpendicular to the direction of tool travel.

Clearance angle, β — the angle between the back of the tool and the work surface.

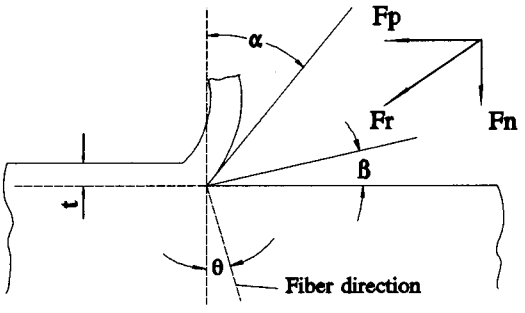

Figure 1. Cutting geometry.

Fiber angle, θ — the angle between the direction of the fiber and a plane perpendicular to the direction of tool travel.

Chip thickness, t — the distance from the original work surface to the new surface being formed by the cut.

Parallel force, Fp — the force component acting in the direction parallel to tool motion.

Normal force, Fn — the force component which is perpendicular to the direction of tool motion.

Resultant force, Fr — the resultant of parallel and normal cutting forces.

Cutting velocity, V — the velocity of the cutting tool relative to the work piece.

Feed — the movement of the work piece resulting in a continuous or intermittent contact with the cutting tool.

2. Orthogonal Cutting

Orthogonal cutting is the machining with a knife whose edge is perpendicular to the direction of tool motion generating a plane surface parallel to the original work surface. Orthogonal Cutting is the most basic form of wood machining and includes such common operations as sawing and planing. Figure 1 shows the geometry of orthogonal cutting. Many wood cutting studies have been conducted using this form because the cutting parameters are easy to control and the cutting forces are easy to measure.

3. Peripheral Milling

Peripheral milling, or rotary cutting, is defined as the cutting with a rotating cutterhead that makes intermittent contact with the work piece moving tangentially to the path described by the tool (Franz, 1958). Usually the rotating speed of the cutterhead is very high, in the order of a thousand revolutions per minute (rpm). Compare to orthogonal cutting, the productivity is higher and the quality of the product is better. For this reason, peripheral milling is widely used in industrial processes. There are many forms of rotary cutting. This thesis only concentrates on the up-milling, of which the feeding direction is opposite to the cutting direction, as shown in Figure 2.

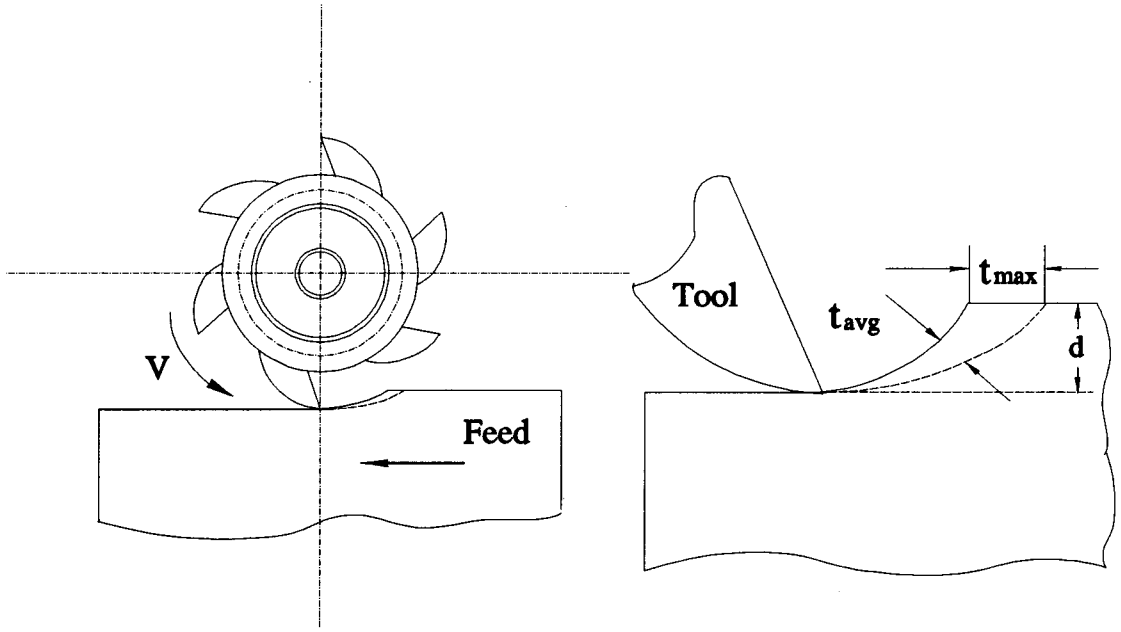

Figure 2. Geometry of Peripheral Milling.

Cutting Path — The cutting path of the tool tip is a trochoid referred to the moving work piece. As the spindle speed increases, the trochoid becomes more circular. Usually the cutting speed is much larger than the feeding speed, so a circular arc can be used to describe the cutting path for simplifying calculations. Actually, the approximation can give very accurate results in most cases (Armarego, 1969; Coombs, 1988).

Cutting Parameters — The main parameters of peripheral milling are described in the following equations. Some are also shown in Figure 2.

The cutting velocity, V, can be described as

$$V = \frac{\pi D n}{60} \quad (inches/second) \tag{1}$$

where D is the diameter of the cutterhead (inches) and n is the spindle speed (rpm).

The feed per tooth, F_t, can be found from

$$F_t = \frac{12F}{Tn} \quad (inches) \tag{2}$$

where F is the feed rate (feet/minute) and T is the number of knives.

The length of path of knife engagement, L, can be shown to be

$$L = \frac{D}{2}\arccos\left(1-\frac{2d}{D}\right) + \frac{F_t T}{\pi D}\sqrt{Dd-d^2} \quad (inches) \tag{3}$$

where d is the depth of cut (inches).

The average chip thickness, t_{avg}, is expressed as

$$t_{avg} = \frac{F_t d}{L} \quad (inches) \tag{4}$$

The maximum chip thickness, t_{max}, is determined by the equation

$$t_{max} = 2F_t\sqrt{\frac{d}{D}\left(1-\frac{d}{D}\right)} \quad (inches) \tag{5}$$

4. Chip Formation

In the finger-jointing process, the cutting direction is perpendicular to the grain direction, known as 90°-90° direction. Only this situation will be discussed here.

McKenzie (1960) studied cutting perpendicular to the grain, and classified the chip formation with two types, as shown in Figure 3. In a type I chip formation, the subchip

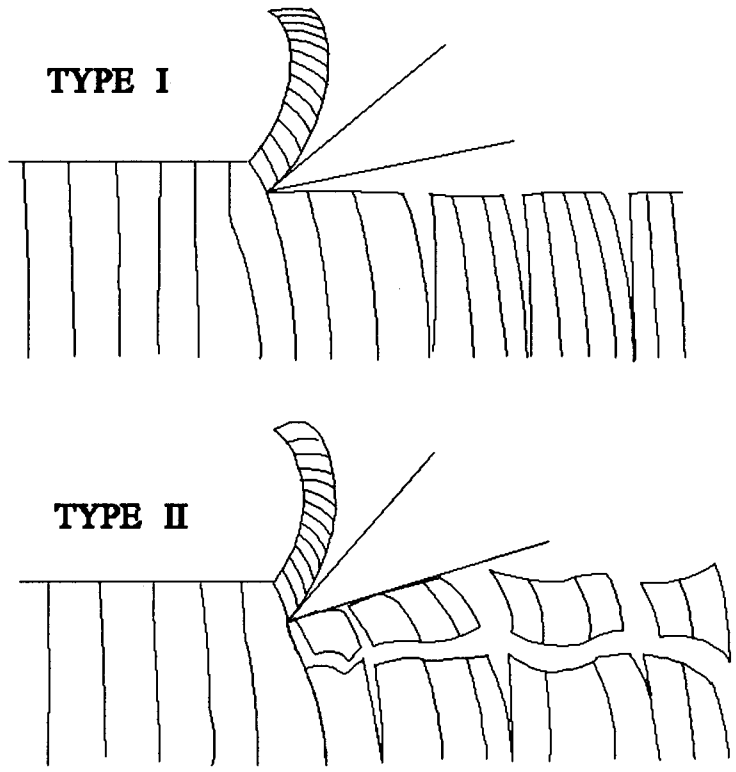

Figure 3. Chip Formations of 90°- 90° Cutting Direction.

is formed above the cutting plane by shear, and loosely linked together. It is found that splits occur along the grain below the cutting plane. Type II failures occur in a plane perpendicular to the grain and parallel to the cutting plane, at a distance below it. Type II may be continuous or intermittent. Chips occur above the cutting plane and below it. This failure type results in a poor surface quality and low cutting efficiency. Figure 3

also shows that the fibers are first bent, and then severed. Failure is caused by tension building in the individual fibers. When the failure occurs, the high tension, built up in the fibers in front of the tool tip, is suddenly released. Then, the chip above the cutting plane is severed into subchips. This is the type I chip formation. In a type II failure, the stress built up a distance below the cutting plane is larger than that in front of the cutting tip, so the failure below the cutting plane occurs before the fibers near the tip are severed. This leads to the chips formed below the tool.

5. Finger-joint and Chip-out

Finger-jointing is a method of joining two pieces of lumber end-to-end by cutting into the end of each piece a set of projecting "fingers" that interlock. Then the pieces are glued together to form a strong joint (Dean, 1978). The most common type used is a horizontal finger-joint, as shown in Figure 4.

The machining of a finger-joint is a peripheral milling process. One of the major defects occurring during machining is chip-out, the breaking of small chips from the trailing edge of the cutting block (Figure 5).

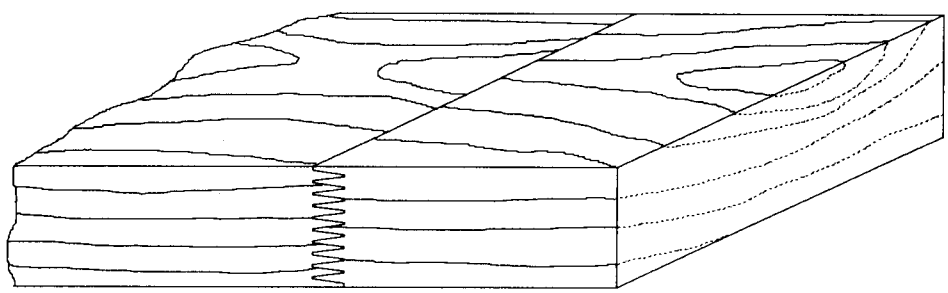

Figure 4. Horizontal finger-joint.

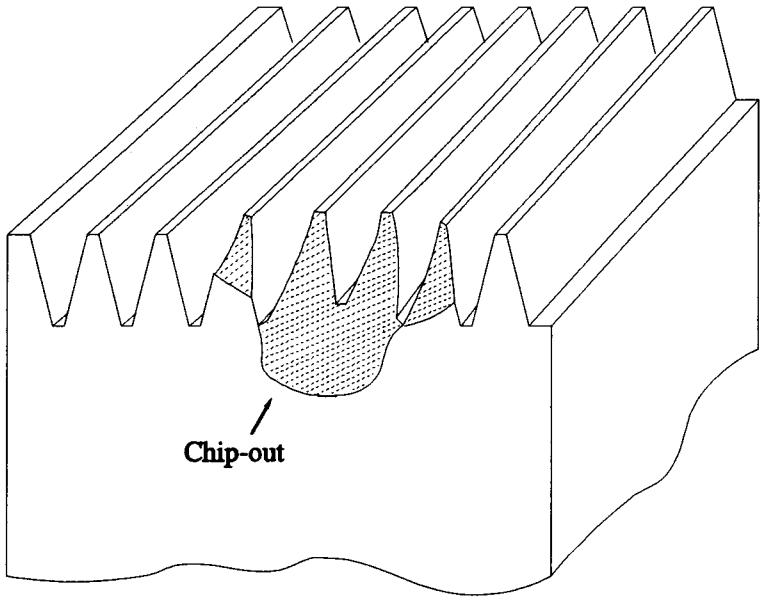

Figure 5. Finger-joint block with chip-out.

To investigate the causes of chip-out, research was started at Oregon State University's Department of Forestry Products by Malcolm Coombs (1988). The orthogonal cutting method was used in his studies to build a chip-out model, and to estimate the cutting forces in the peripheral milling of finger-joints in Ponderosa Pine cutting stock. Coombs found that the fiber inclination and the chip thickness were the main factors which determined the occurrence of chip-out. Table 1 shows the frequency of chip-out in Coombs' orthogonal cutting tests.

Table 1. The frequency of chip-out in the orthogonally cut test blocks (Coombs, 1988).

Fiber Angle	Chip Thickness (inches)			
	0.005	0.010	0.015	0.020
15°	0%	0%	0%	0%
10°	0%	0%	27%	40%
5°	0%	55%	75%	80%
0°	50%	78%	90%	100%
-5°	63%	82%	100%	100%
-10°	64%	97%	100%	100%
-15°	100%	100%	100%	100%

By using a logistic regression software, Coombs also found a formula for chip-out frequency to be

$$frequency = \frac{e^{-1.598+239.9t-0.3216FA}}{1+e^{-1.598+239.9t-0.3261FA}} \quad (6)$$

where FA is the fiber angle (degrees), and t is the chip thickness (inches). Coombs concluded that chip-out always occurred when the angle between cutting force and the fibers was greater than 75° and ceased when this angle was below 55°.

6. Cutting Force Measurement

There are many types of force measuring devices. Beam type dynamometers and force plates are commonly used in cutting force measurement (Figure 6) (Loewen, 1951; Clarke, 1963).

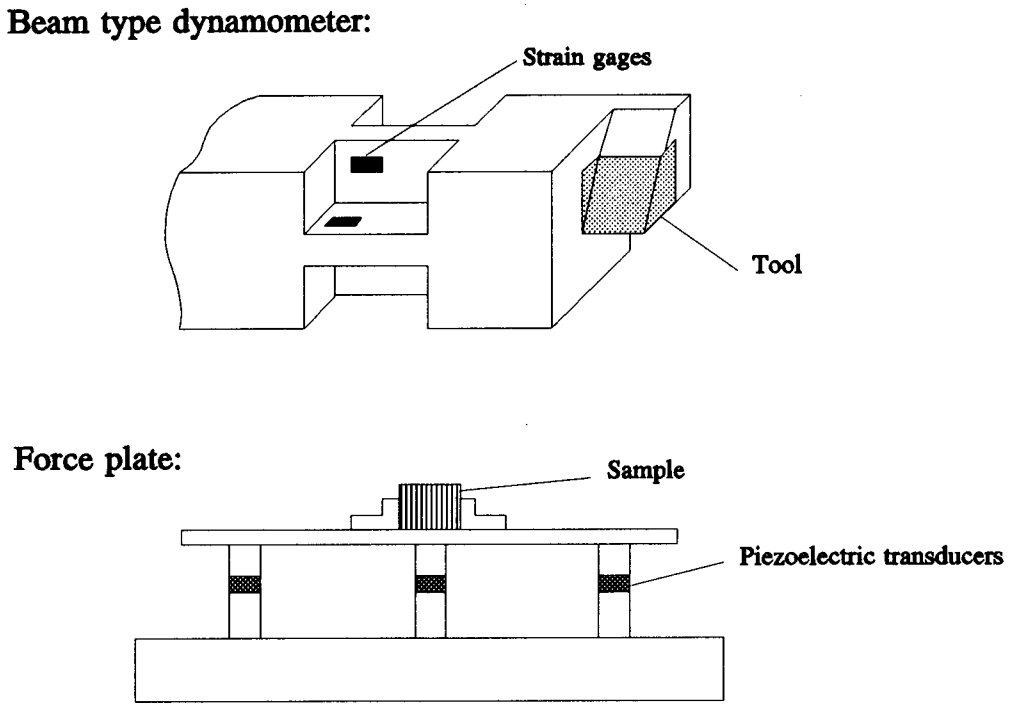

Figure 6. Two types of dynamometers.

The beam type dynamometer measures the forces in two directions, and the force plate can measure in three directions. The sensors can be strain gages or piezoelectric transducers. Calibration is needed for both cases. The dynamometer using strain gages can be calibrated with dead weights. Piezoelectric transducers may be calibrated with the sudden release of dead weights (Axelsson, 1991).

7. Cutting Force Model

McKenzie (1979) conducted an experiment of 90°-90° direction cutting and recorded the cutting forces. The results indicated that the cutting force revealed small regular fluctuations of a type I failure. In a type II failure, the cutting force oscillated

regularly with a long wave length. The oscillation was associated with the fluctuation in the distance of the failure zone. Coombs (1988) found the cutting forces fluctuated as the knife moved across the block. Figure 7 shows a typical cutting force readings for a single pass of the tool. The parallel force was found to increase linearly with each pass due to the cutting length of the bit sides. The normal force remained steady in each pass. This indicated that the parallel force was caused by both the tip and the sides of the tool, while the normal force was almost entirely due to the cutting action of the tool tip.

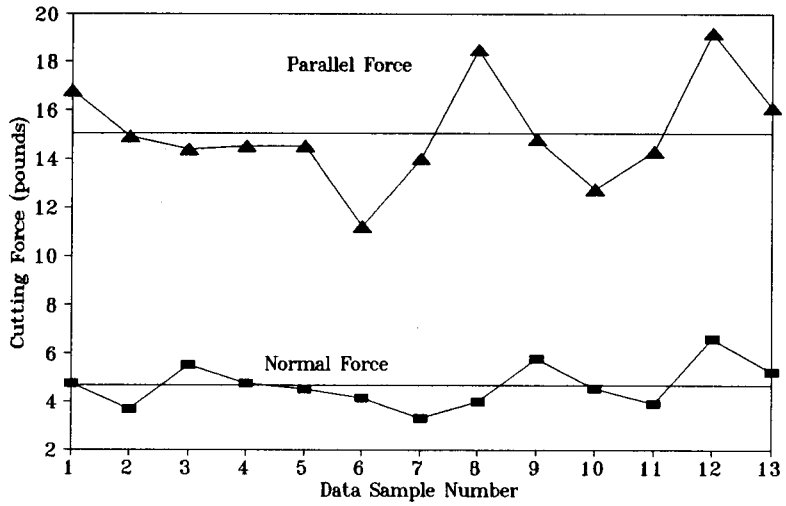

Figure 7. Coombs' (1988) typical cutting force recordings for a single pass.

Coombs' research showed that the chip thickness was the main factor that effected the cutting forces. The specific gravity was found to be the next most important variable in determining the cutting forces. Fiber angle had a very minor effect which was difficult to measure in the tests.

By using linear regression, Coombs derived the equations for calculating the cutting forces, as shown in Equations 7.

$$Fp=(64.6SG+893.0t-11.0)l+(1188.0t+8.0)SG+(-317.0t-2.0)$$

$$Fn=(-336.8t+7.1)SG+(-1.42t+0.0084)FA+(147.4t-1.35)$$

$$Fr=(Fn^2+Fn^2)^{1/2} \quad (7)$$

where t is the chip thickness (inches), l is the length of the tool cutting side (inches), and SG is the specific gravity of the wood.

A cutting force model of peripheral milling was extrapolated based on this orthogonal cutting model. This model predicts that the cutting force will reach a maximum near the point when the tool just makes contact with the cutting block, and then decrease sharply. The chip thickness increases linearly from zero to the maximum. It assumes that the sides of tool are significant in determining the magnitude of the cutting force. At zero chip thickness, only the friction of the knives will be felt. Figure 8 shows a graph of predicted cutting force model of peripheral milling with a single tool bit. The chip acceleration forces were not considered. Verification was not attempted in Coombs' research due to the technical limitation of the equipments.

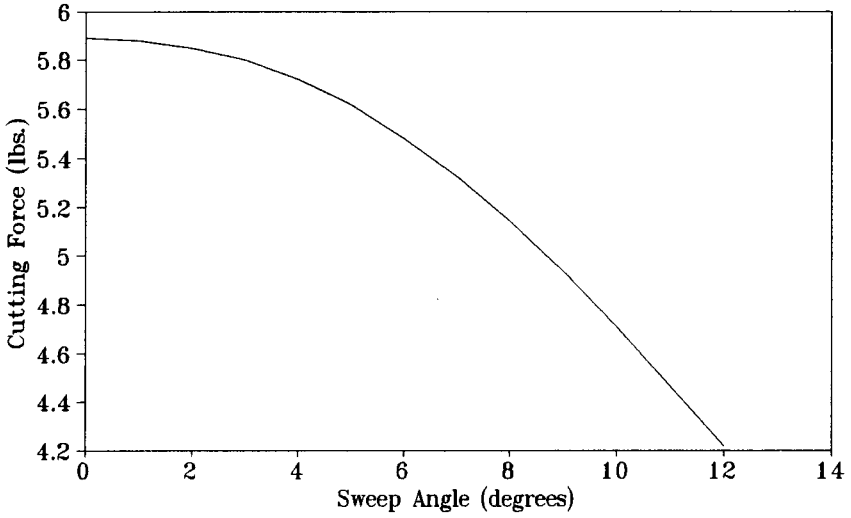

Figure 8. Coombs' (1988) predicted cutting force model of peripheral milling.

III. METHODS AND MATERIALS

1. Typical Finger-jointing Conditions

With the support of a manufacturer, two cutterheads were used in this project. The cutting diameter is 8.75 inches. There are six knives per head. Each knife has eight tool bits bolted together. The rake angle is 22 degrees. In industry, finger-jointing typically operates under the following conditions: the spindle speed of the cutterhead is 3600 rpm, feeding speed of cut-block is 65 feet/minute, finger length is 0.25 inches, and the maximum chip thickness is 0.01 inches (Coombs, 1988).

In this research, the test conditions were set as close as possible to that in industry. The force measuring device was designed based on these dynamic conditions.

2. Data Acquisition

A IBM-XT personal computer with a data translation board was used in the tests. The board, DT2801A, made by Data Translation and modified by HP, is a 16-channel, ADC/DAC board. The maximum data sampling frequency is 27,500 Hz (samples per second). If two channels are used, the maximum sampling frequency is 13,750 Hz for each channel. With this sampling speed, the maximum signal frequency is limited to about 600 Hz.

The operation of the board is controlled by programs written in C or BASIC. The analog signal is first converted into digital data, and stored in the RAM. Then, the

data can be processed and saved in the hard disk for further uses. Due to the limitation of the data storage, the maximum number of data points for each measurement is 21,000. This gives a period of about 0.7 seconds measuring time at the maximum sampling rate for two-channel recording.

3. Design of Dynamometer

The design of the dynamometer needs to incorporate sufficient frequency response and sensitivity for this particular dynamic application. In this case, forces are quite low, on the order of 5 pounds, and signal frequencies of several hundred Hertz or more are expected.

As discussed before, there are primarily two types of dynamometers, the beam dynamometer and the force plate. The force plate can measure forces in all three directions and is basically a plate resting on load cells. The mass of the plate could be fairly large. The dynamic model of the force plate can be regarded as a mass, M, supported by a spring with a spring constant K. The natural frequency of the system is described as:

$$frequency = \frac{1}{2\pi}\sqrt{\frac{K}{M}}, \ Hz \qquad (8)$$

If the mass of the system is large, the natural frequency will be low. In other words, the frequency response of the force plate is usually low. When the signal frequency is close to the natural frequency of the measuring device, it will cause the system to vibrate seriously so that the real signal is difficult to evaluate.

A beam type dynamometer only detects forces in two directions which is adequate for this research. The cutting force analysis is based on the force components in the direction parallel and perpendicular to the feeding direction. Because of the symmetry of the tool bits, the cutting force transverse to the feeding direction is so small that is not of interest in this project.

The beam dynamometer can be designed so that it is small in size, light in weight, and simple to fabricate. The beam could be a tube, a solid cylinder, or a square beam. In order to get a high natural frequency, the beam needs to be very stiff. However, the stiffer the beam is, the less sensitive the dynamometer becomes. To increase sensitivity, semi-conductor strain gages can be used instead of foil strain gages. The former are about fifty times more sensitive than the latter.

With all of the above considerations, several different designs were tried and compared. The final design was chosen to be a beam dynamometer with a size of 2.0 $\times$ 1.094 $\times$ 1.094 inches. The beam was made of steel. Four semi-conductor strain gages were located 1 inch from the end on which the wood sample was mounted.

The following sections give the detailed verification and calculation of the frequency response, sensitivity, and calibration of the dynamometer.

Frequency Response - The natural frequency of a cantilever beam can be found from any text on vibrations, for example (Thompson, 1988), and is given as

$$Frequency = \frac{(\beta_n L)^2}{2\pi}\sqrt{\frac{EI}{mL^4}} \qquad (9)$$

where E is the modulus of elasticity (psi), I is the moment of inertia (in^4), m is the mass per unit length ($lb\text{-}sec^2/in^2$), L is the length of the beam, and $(\beta_n L)^2 = 3.516$ for the first mode vibration.

The moment of inertia, I, for a rectangular cross-section beam is given as

$$I = \frac{b h^3}{12} \qquad (10)$$

where b is the width of the beam (in), and h is the height of the beam (in). In the final design, b = h = 1.094 in, resulting in an I equal to 0.119 in^4. Given L = 2 in, E = 30×10^6 psi, and density = 0.00073 $lb\text{-}sec^2/in^4$, the natural frequency of the beam can be found to be 8,940 Hz using Equation 9.

To verify this calculated natural frequency, a experiment was done by applying a impulse on the beam to induce the free vibration. The test results showed a frequency of about 8,400 Hz, which is very close to the theoretical value.

Sensitivity - When a cutting force is applied to the wood block, the bending moment produced on the beam dynamometer results in surface strain detected by the strain gages. The magnitude of the strain determines the

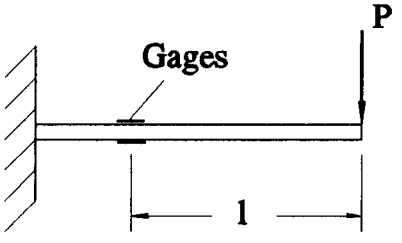

Figure 9. A model of the beam dynamometer.

sensitivity. The dynamometer can be regarded as a cantilever beam, as shown in Figure 9. The cutting force, P, is assumed to be on the order of 5 lb, and the distance between the gage center and the force acting point, l, is 1.63 inches.

By using standard equations of mechanics of materials, the strain, ϵ, at the location of the gage is

$$\varepsilon = \frac{Plh}{2EI} \tag{11}$$

If P equals 8 lb, the remaining known values are substituted into 11, the resulting strain is about 2 μS. This very small strain is very difficult to measure using foil strain gages. To increase output, four semi-conductor gages were connected to form two half bridge (Wheatstone bridge) circuits, measuring forces in two perpendicular directions. The circuits were powered by a Measurements Group strain gage conditioner/amplifier, model 2100 system. The system has an adjustable gain ranging from 100 to 2100, and a bandpass from DC to 5,000 Hz. The strain gages used have a gage factor of 100, and a mounted gage resistance of 133 Ω at room temperature. The response of the semi-conductor gage is described by Equation 12 (Tuppeny, Jr., 1965) as

$$\frac{\Delta R}{R_o} = \left(\frac{T_o}{T}\right) \times \varepsilon \times GF + \left(\frac{T_o}{T}\right)^2 \times \varepsilon^2 \times C \tag{12}$$

where GF is the gage factor, ΔR is the change in gage resistance, R_o is the unstressed gage resistance at T_o, T is the temperature in degrees Kelvin, and C is the nonlinearity constant of the gage.

The second term in Equation 12 is on the second order of the variable ϵ. Since the strain is so small ($\epsilon \approx 2.0\times10^{-6}$), this term can be neglected. Thus, the sensitivity of the gage at room temperature ($T = T_o$) becomes

$$\frac{\Delta R}{R_o} = \varepsilon \times GF = 2\times10^{-6}\times 100 = 0.0002 \qquad (13)$$

In a half-bridge circuit, the output voltage is

$$V_{out} = \frac{V}{2}\left(\frac{\Delta R}{R_o}\right) \qquad (14)$$

where V is the excitation voltage. In this case, V = 4.0 volts and it follows that V_{out} = 0.4 mV. If the maximum gain, 2100, was used in the gage amplifier, the output signal will be on the order of 800 mV.

Calibration - The two channel outputs from the gage conditioner/amplifier were transmitted to the computer using the Data Translation board and recorded as digital data. Through calibration of the system, the data were turned into the values of tool-force components which could be processed or stored. Calibration of the system was accomplished by using a series of weights suspended from a reference point on the cut block where the tool was going to pass. The digital data values versus weights for both channels are plotted in Figure 10. It can seen that the calibration curves are very linear. Thus, neglecting the nonlinearity term of the semi-conductor gage is acceptable in this application.

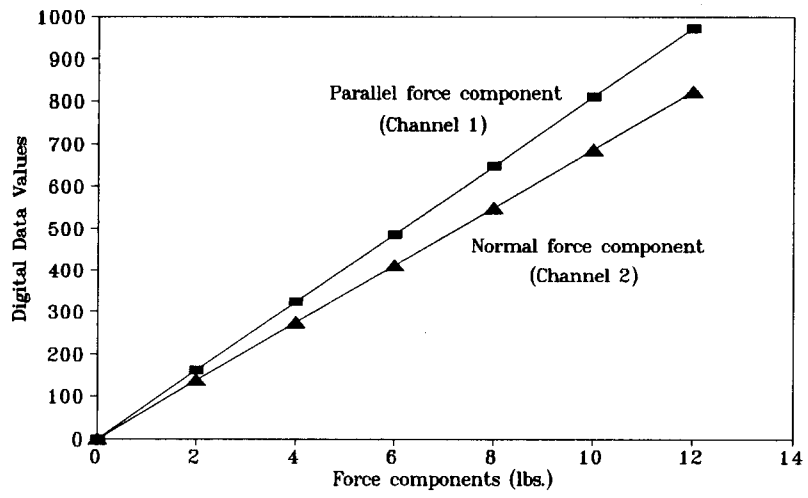

Figure 10. Calibration curves for the dynamometer.

Torsional Effects - The cut test block was mounted on the end of the dynamometer. To minimize the torque caused by the off-center force, the attachment was designed so that the cutting path was located near the center plane of the beam, as shown in Figure 11.

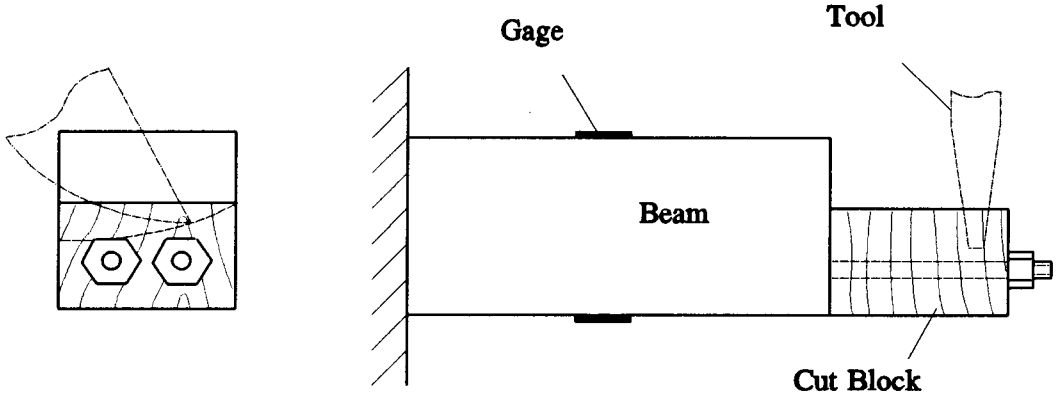

Figure 11. Fixture of cut block on the dynamometer.

However, the action line of the cutting force is not always passing the centroid of the beam's cross-section as the tool tip is traveling across the cut block in a circular arc. Therefore, the torque in the beam can not be totally avoided.

The gages are mounted in the axial direction and insensitive to the shear strain. To verify this, a dead weight was applied on the dynamometer off-centered at a distance of one half the beam's width. This large torsional component was not detectable by the axially aligned gages. Therefore, force measurements should not be influenced by the torsional effects caused by off-center forces.

4. High Speed Video Recording

Finger-joint milling is a relatively high speed operation. The formation of the chip and chip-out happens in a very short time which cannot be observed in real time. High speed video recording provides a means to closely observe cutting details occurring during the processing. A high speed Kodak video recording system was used to record the cutting process by zooming in at the cut block at two different angles. This system is able to record at up to 1000 frames per second, and replays the cutting in slow motion. Two replay speeds of 30 frames/second and 3 frames/second were used. The system is controlled by a IBM-XT computer. The pictures can be dumped on to VHS tapes and reviewed with a VCR. By observing the video recording, the formation of the chip-out and the types of chip can be clearly identified.

5. Sample Preparation

There are many factors that will affect the cutting forces and the occurrence of chip-out, such as species, moisture content, and fiber inclination. The goal is to make the test condition as close as possible to that used in industry. Ponderosa pine is the only species tested in this project. The samples were conditioned to a moisture content of 8

to 12%. The dimension of the sample block were 1.125 × 0.75 × 0.75 inches. The fiber angle was measured with a lumber scribe and protractor. The angle was defined as positive when cutting with the fibers and negative when cutting against the fibers. Groups of samples were made with the fiber angles ranging from 0° to 30°. The sample surface was sanded.

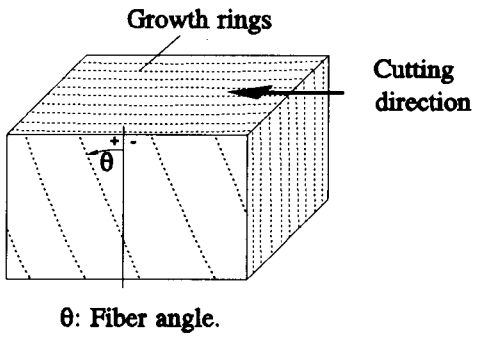

Figure 12. Ponderosa pine sample block.

6. Test Procedure

The cutterhead axis was installed horizontally on a milling machine. Spindle speed was adjustable from 60 to 4200 rpm. The dynamometer was held by a vice on the carriage and was able to be moved in three directions. The movements were displayed by a digital meter with a resolution of 0.0005 inch. A trigger switch was used to set the desired trigger position.

The maximum spindle speed used was 250 rpm due to the limitation of the strain gage conditioner's frequency response and the Data Translation board's sampling frequency. By choosing a proper feeding speed, the maximum chip thickness can be set to be about 0.01 inch, which is a typical value in industry. The chip thickness is one of the main factors which affects the cutting forces and chip-out occurrence. All tests in this project used the same maximum chip thickness of about 0.01 inch.

Fiber inclination is another main factor that determines the occurrence of chip-out. For chip-out analysis, tests were done with groups of ten samples whose fiber angles ranged from -12° to 12° with an increment of 3°. The spindle speed was set at 144 rpm for chip-out analysis.

In the force measurement tests, spindle speeds of 120 rpm and 200 rpm were used. The fiber angles ranged from -30° to 30° in increments of 5°. The data were saved in binary files for later processing.

7. Data Processing

A program was written in QuickBASIC for data processing giving plots of the force curves on the screen for primary investigation. A "zoom in" function allows more detailed observation at different segments of data, which then can be saved in separate files for further analysis or a final plot.

In some cases, the impact during cutting may induce vibration of the system. This frequency is usually much higher than the force signal frequency. By using a data averaging technique, a low-pass digital filter was put into the program. The window width of the data averaging can be varied to get the desired bandpass. The proper choice of the window width can eliminate the induced vibration signal and leave the real cutting force signal unchanged. Figure 13 shows the cutting force signals mixed with the induced vibration signal. Figure 14 is the signals after filtering. Only the parallel force signal was filtered.

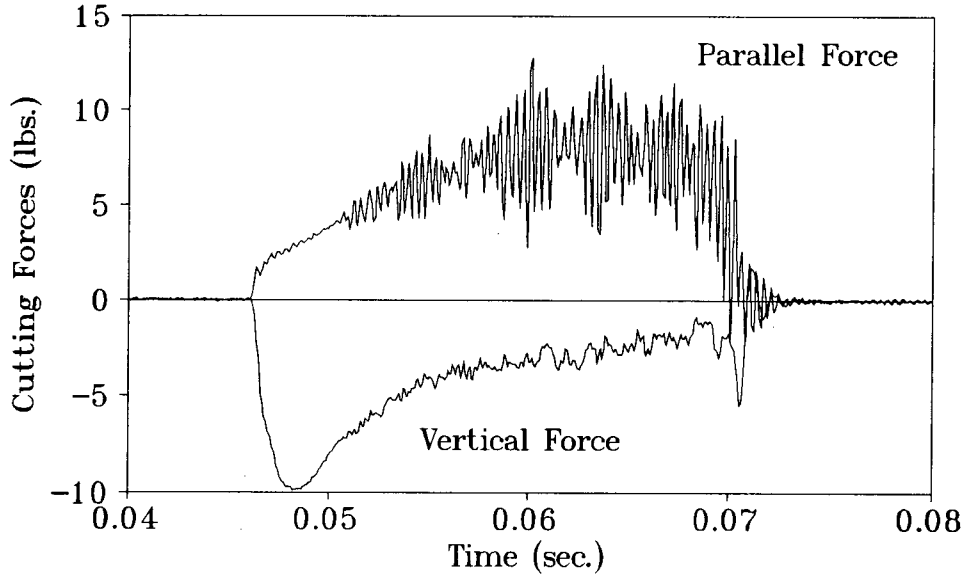

Figure 13. Original Cutting force recordings.

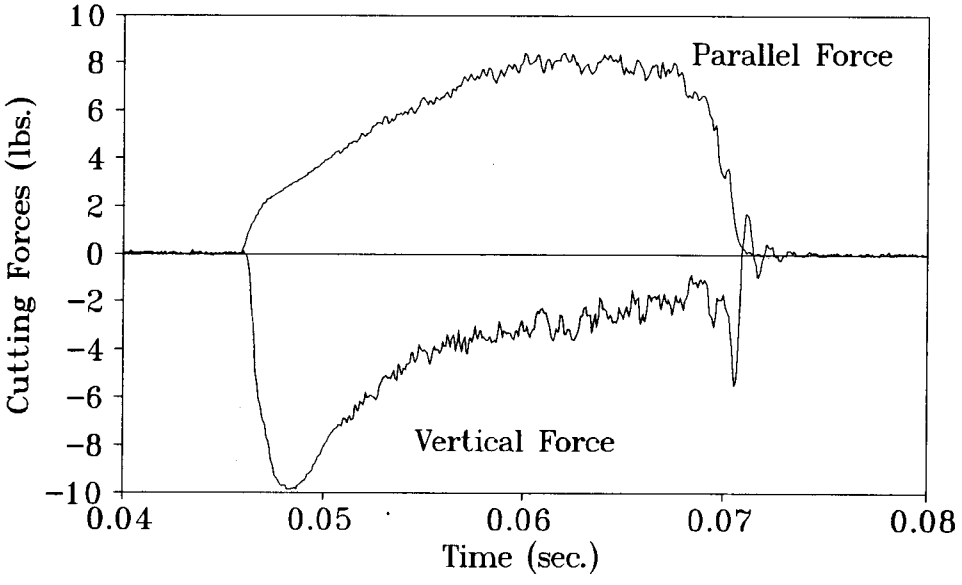

Figure 14. Cutting force signals after filtering (only parallel force signal filtered).

IV. RESULTS AND DISCUSSION

1. Cutting Force Measurement

To verify the force measuring system, a wood sample was cut against the growth ring. Figure 15 shows the real time cutting force history for a single tooth passing through the sample block. The parallel force is the cutting force component in the direction of feed while the vertical record is the force component in the perpendicular direction. A negative vertical force indicates the pressure of the tool on the wood block, and the positive value presents a force tending to pull the block up. The parallel force is obviously larger. The large cyclic frequency of the parallel force varied at a period which was found to closely agree with the distribution and width of the growth rings. This indicates that the cutting force is strongly influenced by the density of the wood as might be expected.

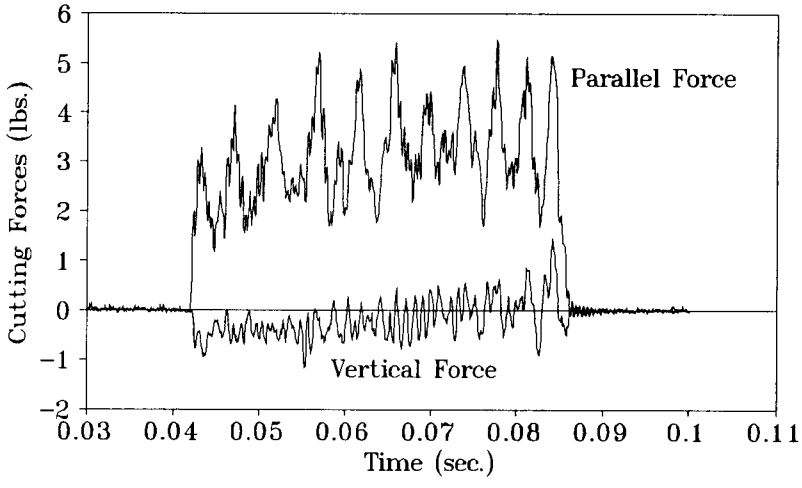

Figure 15. Force recording of a cut against the growth rings.

A plastic sample was also cut for comparison with the wood sample. The force recording is shown in Figure 14. The hardness of the plastic is much higher than the

wood. It was found that the vertical force was relatively large in this case, indicating that the vertical force is more sensitive to the hardness of the material. Since the plastic has a uniform density, the force curves are quite smooth compared to that recorded in wood cutting. The small fluctuations of cutting force are associated with the different stages of failure in the chip formation.

These test results indicate that the dynamometer design is sensitive enough to measure small force changes due to the density variation and chip formation.

2. Cutting Force Model

Thirty samples with different fiber angles were tested under three spindle speeds: 50 rpm, 100 rpm, and 250 rpm. The maximum chip thickness was all controlled to 0.01 in. As the cutterhead rotated, six tool bits on the circumference made contacts with the sample sequentially.

Figure 16 shows a force record when a single tool bit cut through a wood sample with a fiber angle of -5°. The spindle speed was 50 rpm. Compared to Figure 15, the force curves do not show large periodical fluctuations, because the cut is along the growth rings. However, the force variations are still quite large, since the density is not even in the wood and the growth rings are not exactly aligned with the cutting path. In addition, the chip formation is not a continuous process as discussed previously. Type I failure was observed in all the tests. It was found that the cutting forces varied in different patterns when cut with a different tool bit. The following section will discuss

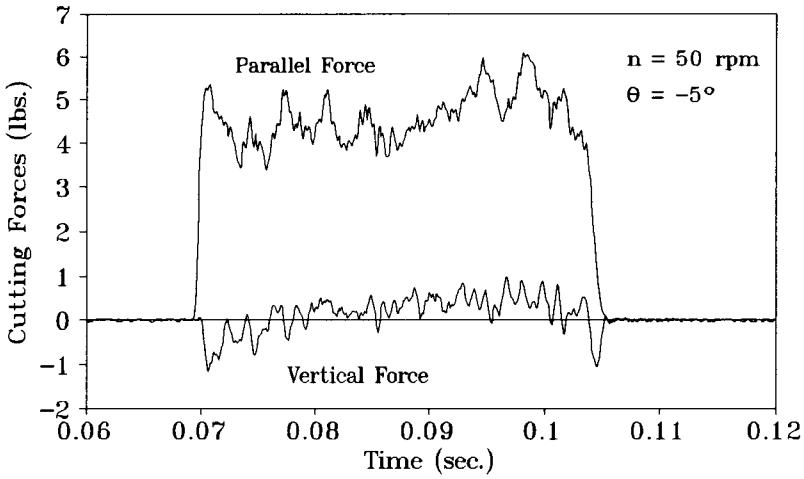

Figure 16. Force recording of a cut as a single tooth passed through the sample. the behavior of the cutting force pattern.

Force Pattern - Figure 17 shows an example of a force recording when the cutterhead rotated more than one revolution. Six teeth on the circumference passed through the wood block sequentially. The recording started when the first tooth made a contact with the sample, and stopped after the first tooth made a second contact with the sample. The fiber angle was -5°, and the spindle speed was 100 rpm.

The time history of force recording showed that the first tooth had very similar cutting force patterns in the first and second contacts with the sample, with about the same maximum magnitude and time variation. However, the maximum magnitudes of the cutting forces varied considerably from tooth to tooth. Moreover, the cutting forces changed in totally different ways when cut with different tool bits. Some tended to increase during a pass, some might decrease or increase first and then decrease. Some teeth tended to press the sample down while others might pull the sample up.

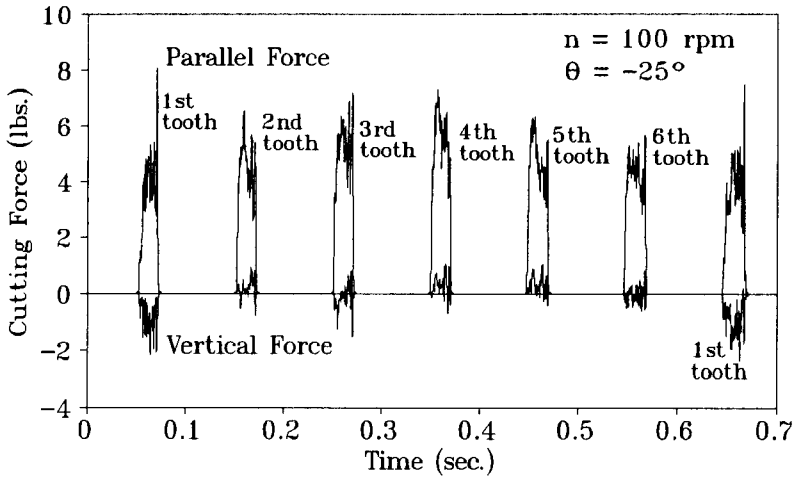

Figure 17. Force recording of a cut at 100 rpm, with a fiber angle of -5°.

Considering the fact that the tool bit cuts the finger-joint with tip and two side edges, additional tests were conducted and the forces were examined when the samples were cut with tool sides only. Figure 18 shows a side cutting force recording when seven tool bits passed the sample sequentially.

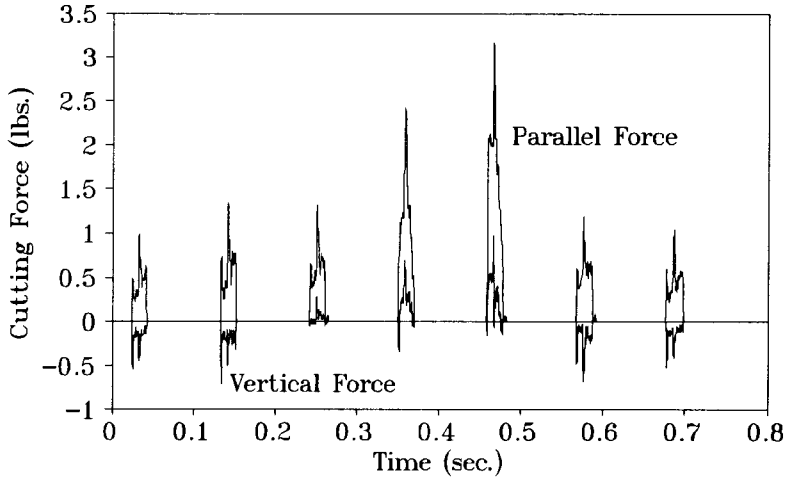

Figure 18. Force recording of a cut with tool sides only.

The results showed that the magnitudes of the cutting forces were relatively small

compare with the normal cutting forces, as shown in Figure 15. This implies that the major cutting forces were caused by the tip cutting of the tools.

Since the tool bits can not be made exactly the same, there are some differences in the shape between the different teeth. These minor differences in shape, such as clearance angle and the width of the tool tip, will cause some teeth to have greater tip cutting than others. Also precise radial position is difficult to achieve which affects tooth to tooth force histories.

Multi-teeth Cutting - As described before, there are six knives on the cutterhead and each knife has eight teeth bolted together. The actual finger-jointing with this cutterhead will form eight fingers on the end of the wood block. A multi-tooth cut was made to examine the cutting force behavior. Three tool bits were used on each knife, so there were three fingers made on the specimen. The force results are shown in Figure 19.

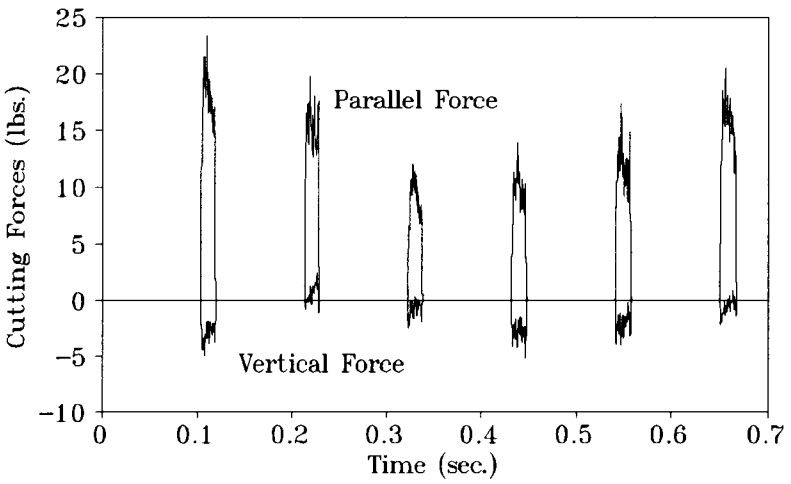

Figure 19. Transient force for three tooth cutting.

The cutting forces shown in Figure 19 is the total cutting forces produced by three

sets of tool bits. As expected, the magnitude of the cutting force is three times of that cut with one tooth. The interaction between tool bits was not found. It was noticed that the average force magnitudes for the series of knives oscillated one cycle when the cutterhead rotated one revolution. This may due to the off-center of the cutterhead. It can be concluded that the total cutting forces in multi-teeth cuts is more sensitive to the radial positioning of the knives, rather than the shapes of individual tool bits.

Cutting Forces at Different Fiber Angles - Cutting forces were examined when the sample blocks with different fiber angles were cut. Figure 20-31 show the results of the cuts with a single tooth at the rotary speed of 50 rpm. Fiber angles are 30°, 5°, 2°, 0°, -2°, -5°, -15°, -20°, -25°, and -30°, respectively. The maximum chip thickness was controlled at 0.01 inches.

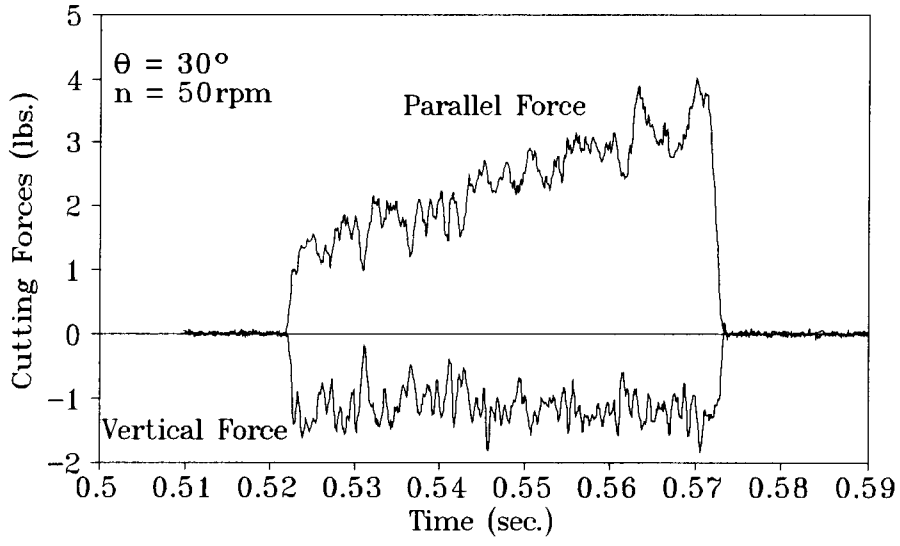

Figure 20. Cutting force recording of single tooth cut with a fiber angle of 30°.

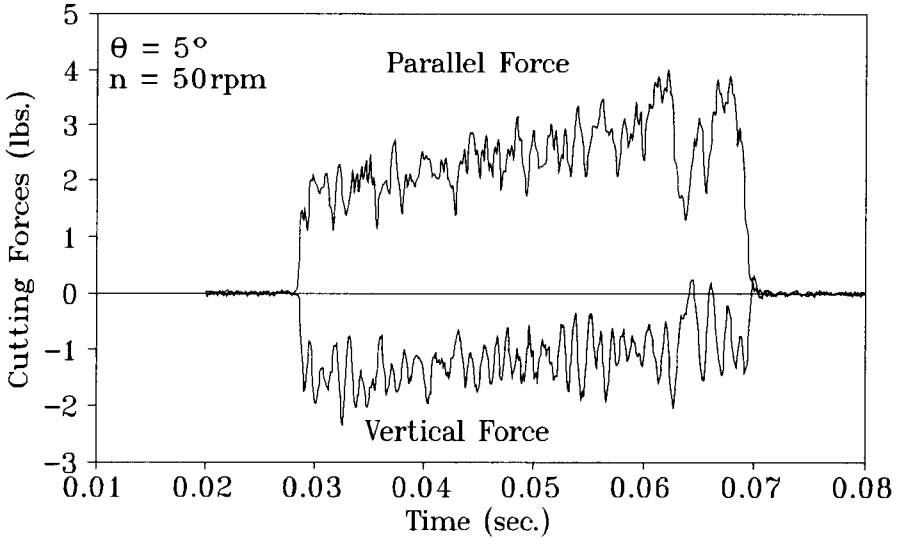

Figure 21. Cutting force recording of single tooth cut with a fiber angle of 5°.

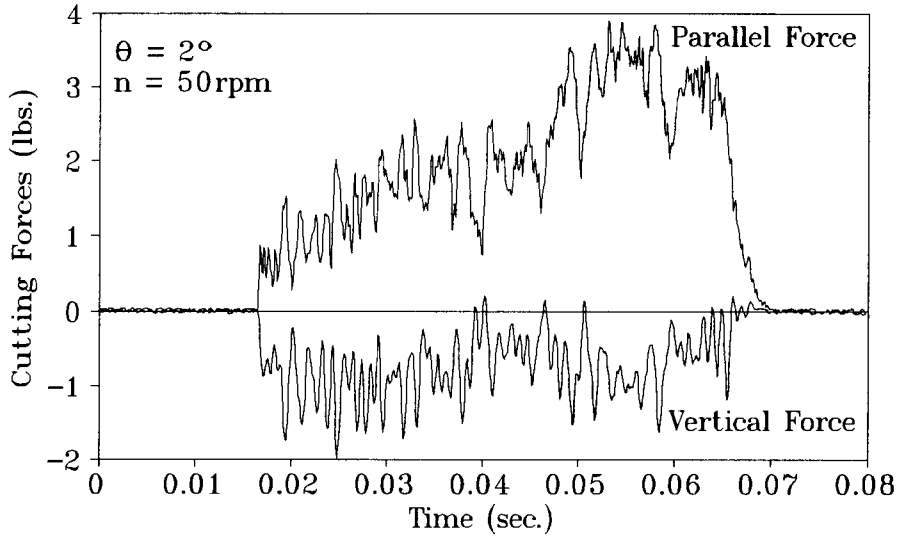

Figure 22. Cutting force recording of single tooth cut with a fiber angle of 2°.

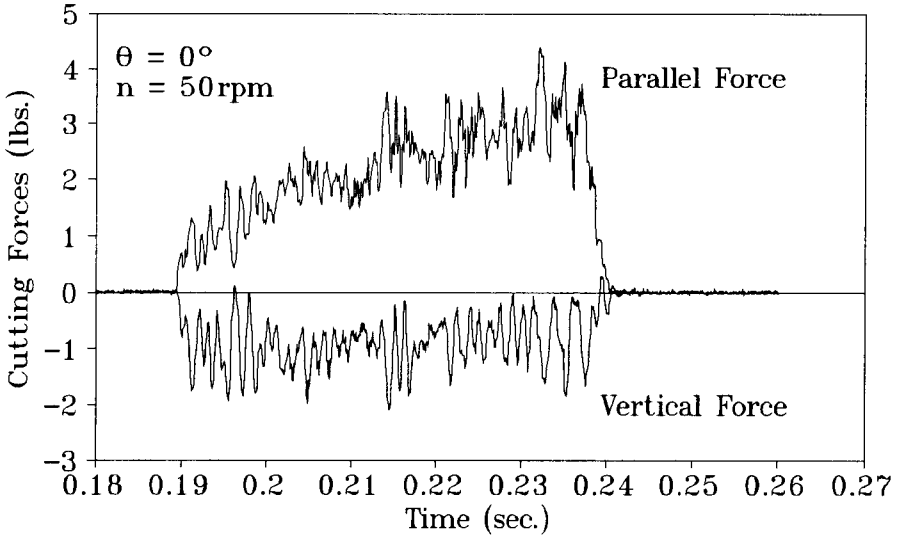

Figure 23. Cutting force recording of single tooth cut with a fiber of 0°.

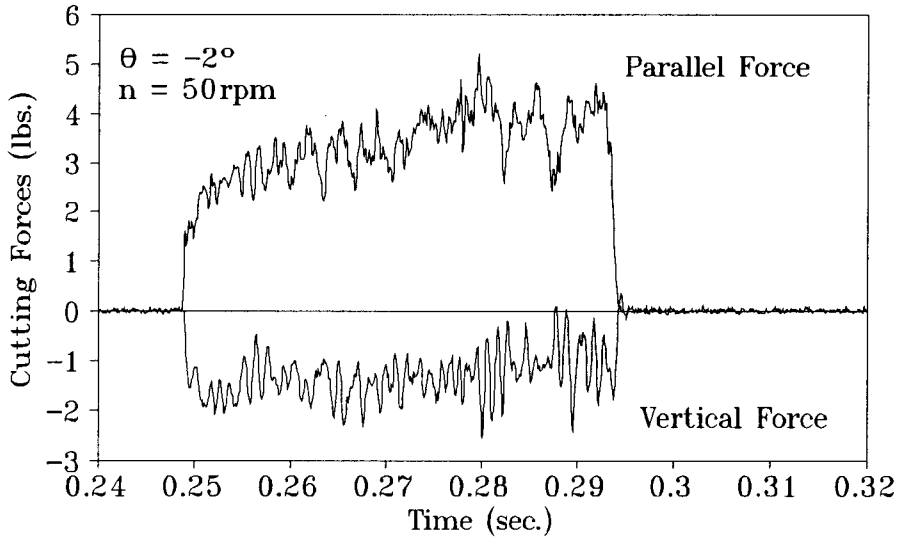

Figure 24. Cutting force recording of single tooth cut with a fiber angle of 2°.

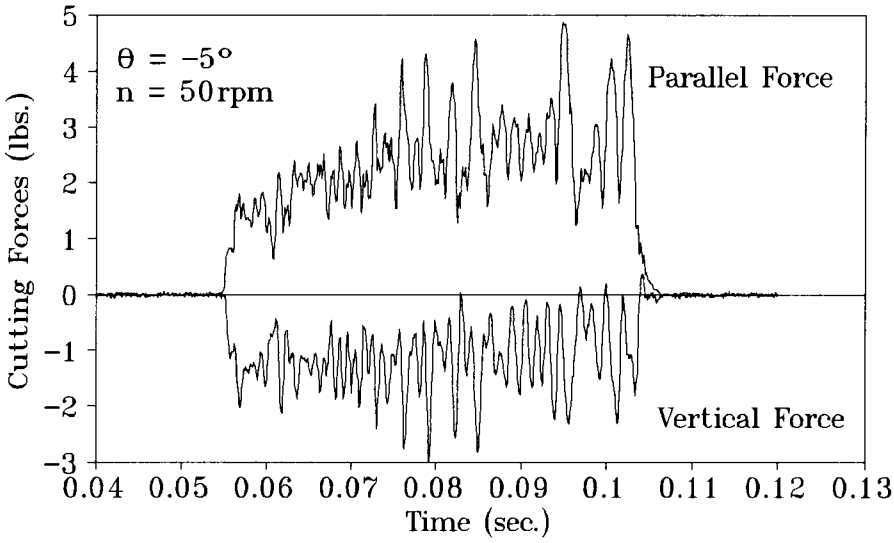

Figure 25. Cutting force recording of single tooth cut with a fiber angle of -5°.

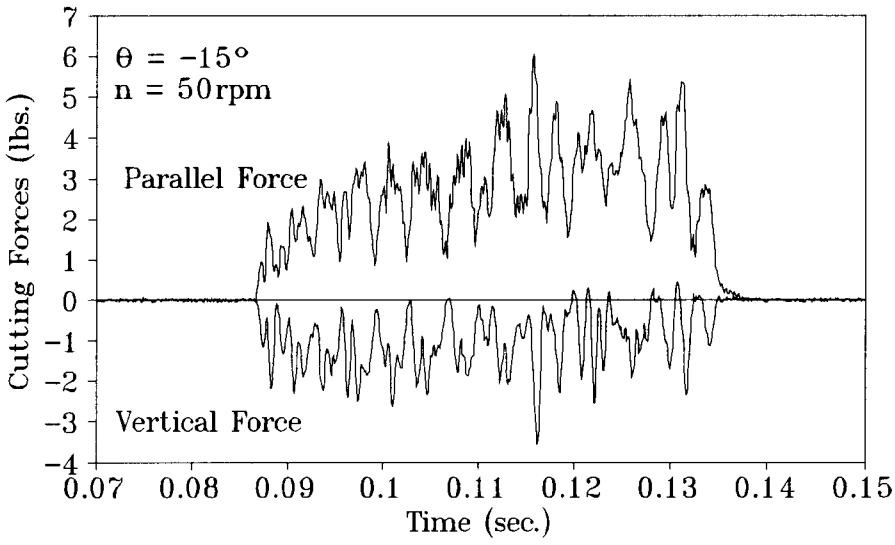

Figure 26. Cutting force recording of single tooth cut with a fiber angle of -15°.

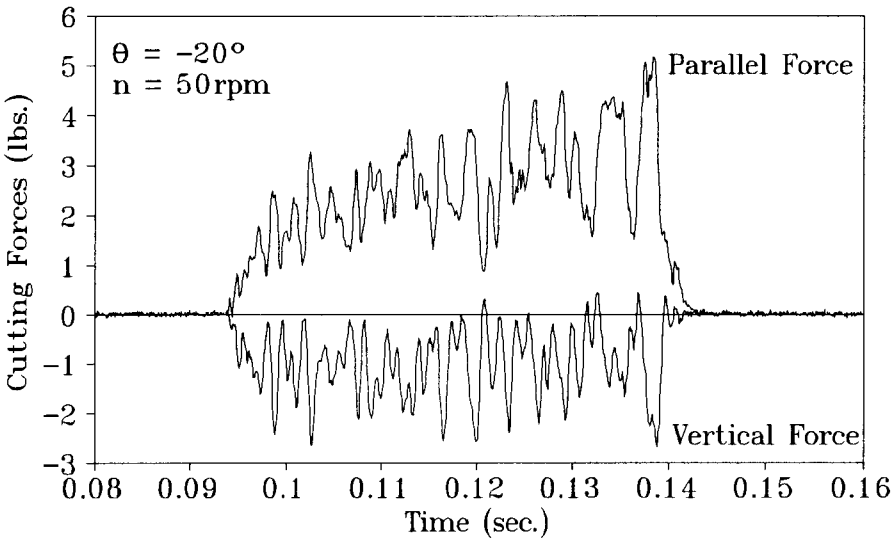

Figure 27. Cutting force recording of single tooth cut with a fiber angle of -20°.

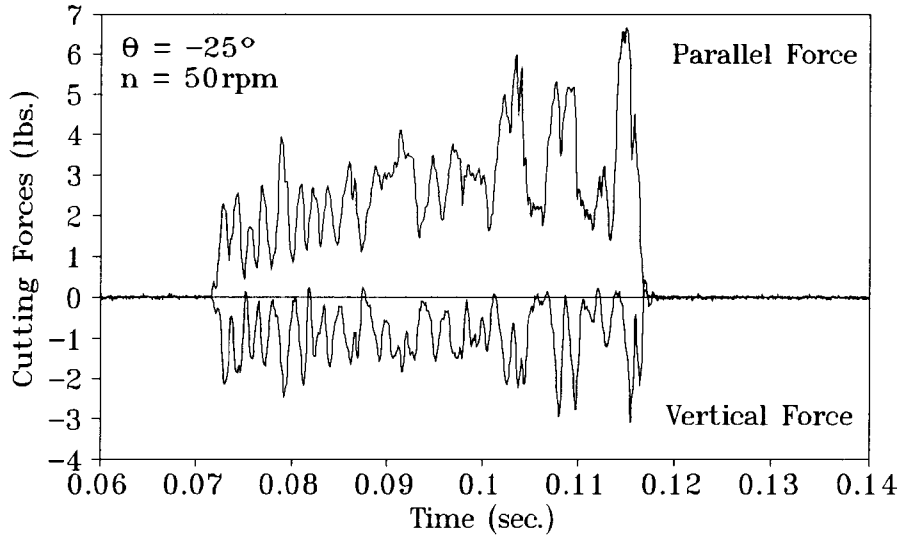

Figure 28. Cutting force recording of single tooth cut with a fiber angle of -25°.

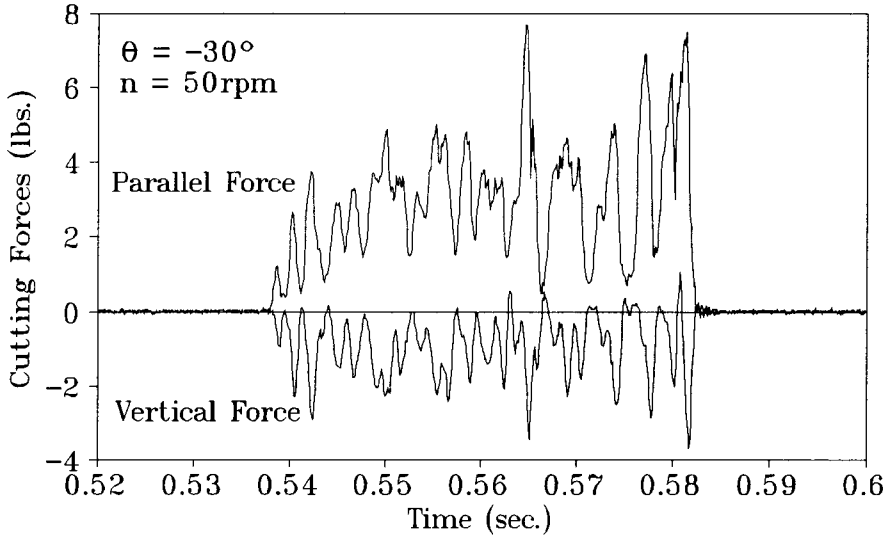

Figure 29. Cutting force recording of single tooth cut with a fiber angle of -30°.

Since the cuts were made with one particular tooth, the cutting force patterns were similar. The vertical force fluctuated at a negative value for all the cases, while the parallel force oscillated in a similar pattern and tended to increase as the tooth passed through the sample. By using linear regression, the average forces were analyzed while the tool passed through the sample blocks at different fiber angles. The average forces versus fiber angle is plotted in Figure 30. The regression curves are shown as heavy lines.

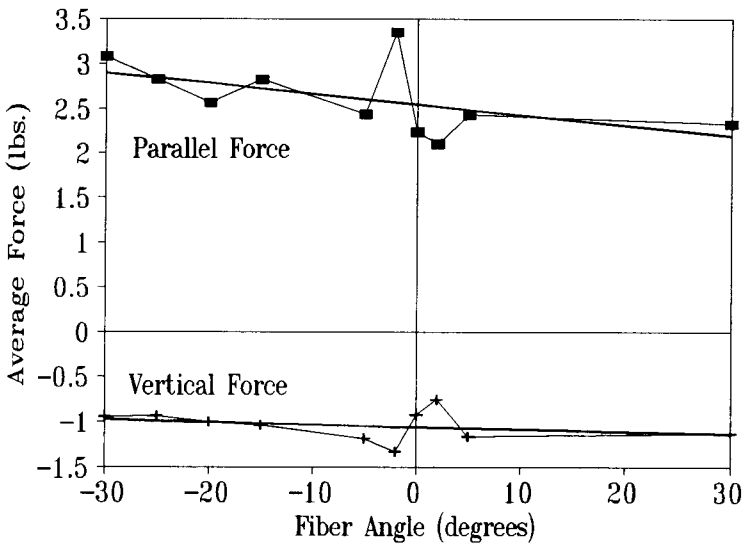

Figure 30. Average cutting force versus test sample fiber angle.

It can be seen that the average parallel force decreases from about 2.9 pounds to 2.2 pounds when the fiber angle increases from -30° to 30°. The fiber angle has a minor influence on the average vertical force, which showed slight increase in the absolute value when the fiber angle increases. The resultant cutting force declined when the fiber angle was increased. In other words, cutting forces increased when cut against the fibers.

The standard error of the average forces were also examined versus the fiber angle. Figure 31 shows the standard error of the average forces at different fiber angles. The regression curves are also plotted as heavy lines.

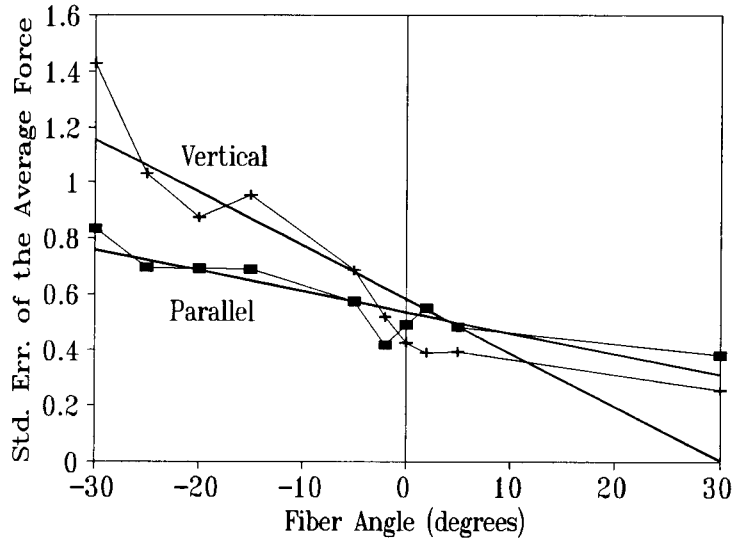

Figure 31. Standard errors of the average forces versus test sample fiber angle.

The results show that the standard errors of average cutting forces are much larger at negative fiber angles than that at positive angles. This implies that the fluctuation of the cutting forces decrease when the fiber angle changes from negative to positive. By observing the quality of the cutting surface, it was found that the cutting surface quality was higher at positive fiber angles than that at negative angles. More serious failures occurred when cut against the fibers, which led to larger variations of the cutting forces.

Several samples were cut with different chip thicknesses. The results agreed well with Coomb's research (Coombs, 1988). No intensive analysis in this area was attempted in this project.

3. Chip-out Model

By reviewing the video recording in slow motion, the formation of chip-out could be clearly observed. The progress can be divided into three stages:

1) As the cutting front approached the trailing edge, a first crack occurred in front of the tool tip when the knife was passing through the corner of the sample block, as shown in Figure 32. The crack closed after the knife swept through, while the crack line is still visible (Figure 33). **2)** When the second knife passed the corner, the crack was enlarged, and the chips were split from the corner, connecting to the block at one end (Figure 34). **3)** In the following contact with the knives, the chips were bent over and the connected end was cracked, as shown in Figure 35.

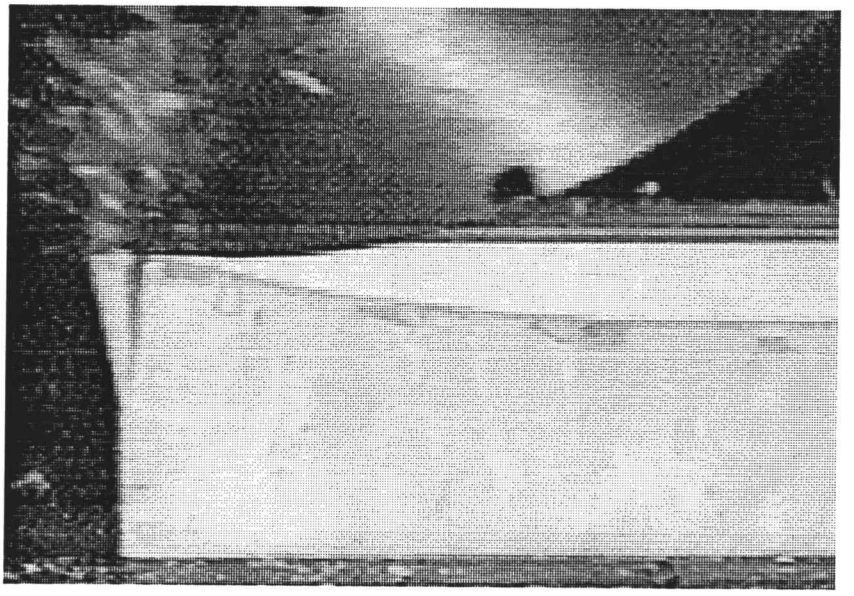

Figure 32. First stage of chip-out formation, with the knife passing through the trailing edge of the wood block.

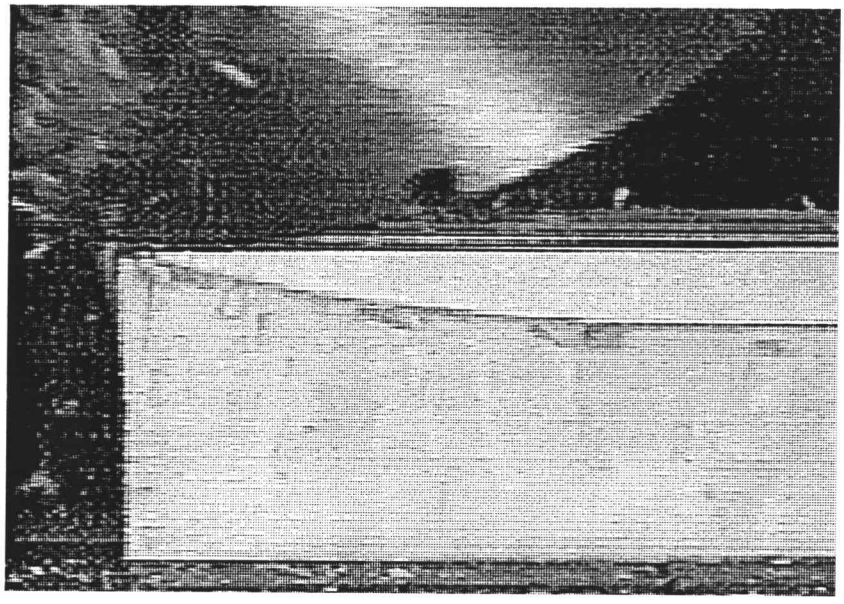

Figure 33. First stage of chip-out formation, after the knife passed through the trailing edge of the wood block.

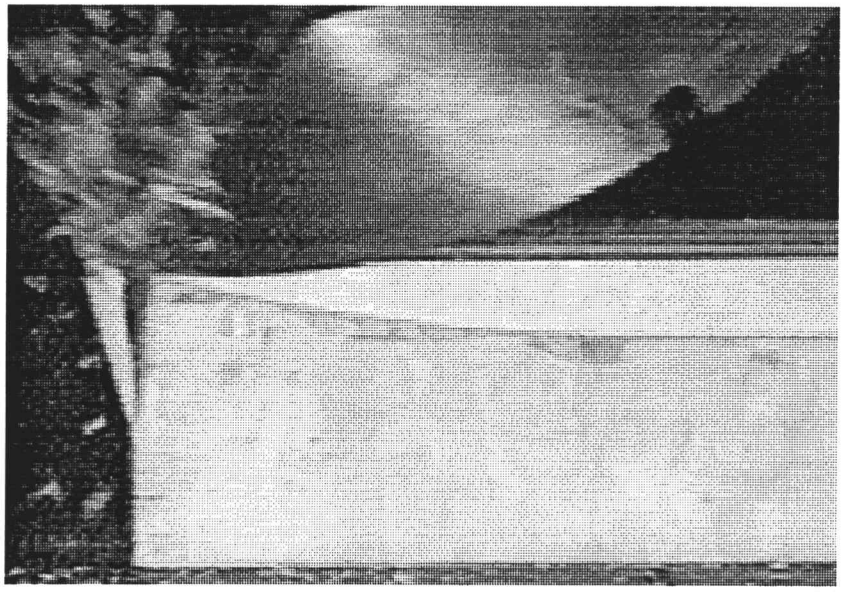

Figure 34. Second stage of chip-out formation.

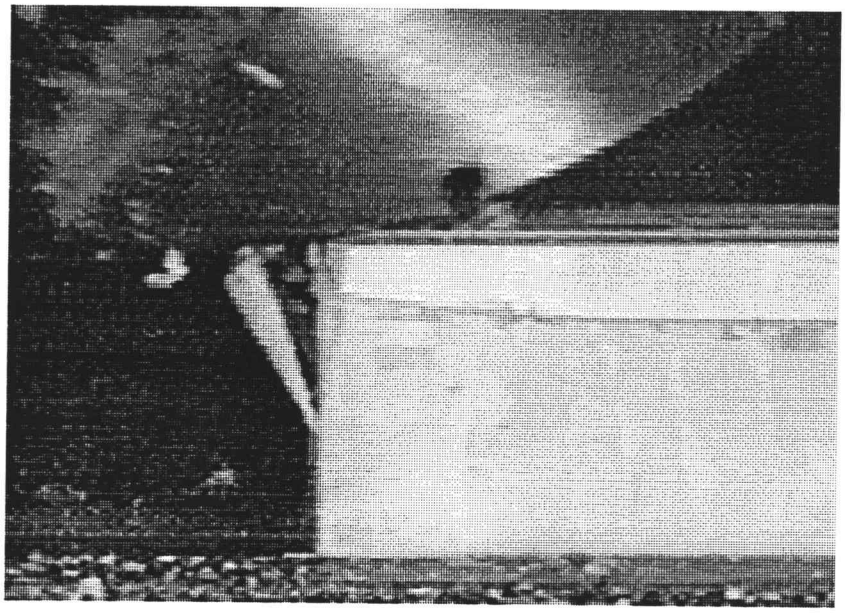

Figure 35. Third stage of the chip-out formation.

It was found that the cracking surface was always lying in the fiber direction. This indicates that the failure occurs along the fibers and implies that the strength of the wood is weak in this surface. By observing the crack surface, it is found that there are light marks shown in transverse directions to the fibers. These are the ray cells. It is the ray cells that weaken the bonds between the longitudinal fibers. The area of the cracking surface varied from sample to sample and also related to the differences of the fiber angles. Larger negative fiber angles tended to result in a larger chip-out. Figure 36 shows the geometry of the chip-out for two different fiber angles. Assuming that the cracking areas are the same in both cases, it can be seen that the volume of chip-out is larger when the fiber inclination is greater, because the cracking surface always lies in the direction of the fiber.

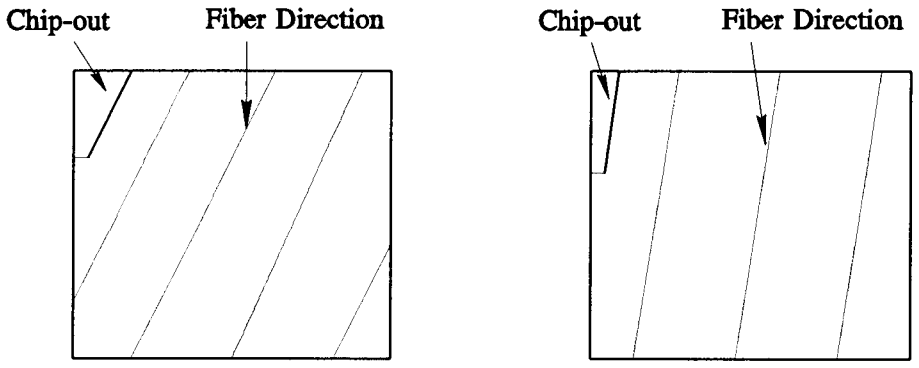

Figure 36. Geometry of chip-out in different fiber angles.

Fiber angles were studied to examine the frequency of chip-out. The spindle speed was set at 144 rpm and the feeding speed at 26 in/min. Maximum chip thickness was 0.01 inches. The results are shown in Table 2.

Table 2. The frequency of chip-out in peripheral milling test blocks with the chip thickness controlled at 0.01 inches.

Fiber Angle	Number of Samples	Frequency
12°	10	0%
9°	10	0%
6°	10	10%
3°	10	60%
0°	40	70%
-3°	10	100%
-6°	10	100%
-9°	10	100%
-12°	10	100%

The results of Table 2 show that chip-out always occurs when the fiber angle is less than -3°. No chip-out can be found when the fiber angle is greater than 9°. To compare with Coombs' (1988) results, the same statistic methods were used. The maximum standard deviation of the chip-out frequency was estimated with Equation 15.

$$\textit{Maximum Standard Deviation} = \frac{\max(p\,q)}{N} \qquad (15)$$

where p is the probability of chip out, q equals 1-p, and N is the number of samples. The result is 2.4%. By using linear regression, an equation was found to estimate the frequency of chip-out at maximum chip thickness of 0.01 inches (Equation 16).

$$\textit{Frequency} = \frac{e^{1.94-0.89\theta}}{1 + e^{1.94-0.89\theta}} \qquad (16)$$

where Θ is the fiber angle (degrees). The standard error of constant was found to be 2.701, the standard error of the Θ coefficient is 0.1162, and the correlation R squared is 0.894. Figure 37 shows the chip-out frequency versus fiber angle. The regression curve is plotted as a heavy line.

Chip-out can be avoided by choosing the fiber angle properly. The fiber angle should be larger than or equal to 9° when the maximum chip thickness is controlled at 0.01 inches. Chip thickness is also a main factor that determines the chip-out occurrence. The chip-out model related to the influence of the chip thickness was well developed in Coomb's (1988) research, and was not attempted in this project.

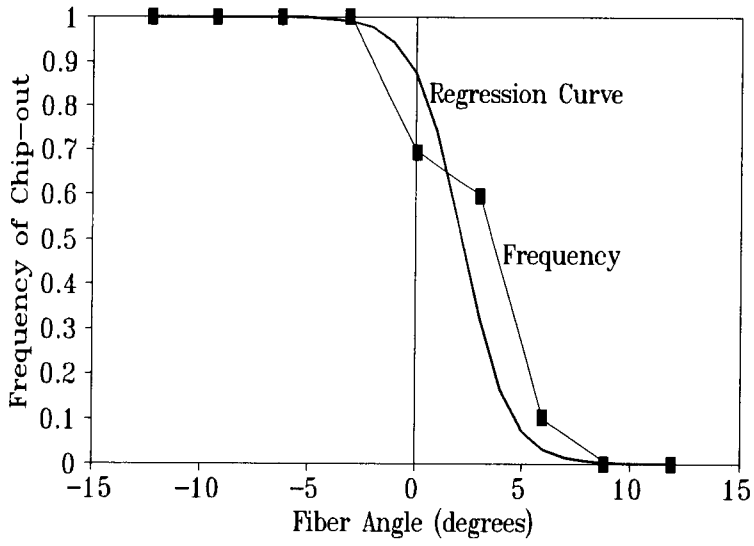

Figure 37. Chip-out frequency of peripheral milling at maximum chip thickness of 0.01 inches.

V. CONCLUSIONS

1. Cutting forces are largely influenced by the density of the wood, as well as the chip thickness. The recorded force curves fluctuate due to the density difference in the wood and the material failure type.

2. The force data indicate that the dynamometer design is sufficiently sensitive to measure the small force changes occurring at high frequencies during the peripheral milling operation. Excitation of the natural frequency of the dynamometer appears to be minimal.

3. The major portion of the cutting force is produced by tip cutting. The vertical cutting force component is mainly caused by the tip cutting, and the parallel force component is a combination of the tip and side cutting of the tool bit.

4. Slight differences of the tool bit shape may result in different cutting behavior for each knife. This leads to the distinct force pattern varying for each tool bit. The balance of the cutterhead and precise radial position of the tool bits also have an effect on the force pattern.

5. Fiber angle has some affect on the cutting force. When cutting against the fibers, cutting force increases slightly and the force fluctuation is larger, accompanied by a poorer surface quality.

6. Chip-out formation is a process of intermittent failure development near the trailing edge of the cut block. The first crack occurs when a knife passes through the edge, and the failure develops in the sequel cuts. Crack surfaces are always lying in the fiber direction.

7. Fiber angle and chip thickness are the determinants of the chip-out occurrence. In the typical finger-jointing operation with maximum chip thickness of 0.01 inches, chip-out occurs when the fiber angle is less than -3°, and no chip-out is observed when the angle is greater than 9°. Properly orienting the fiber can avoid the occurrence of chip-out.

8. While the dynamometer performed satisfactorily, no evidence was found that the chip-out has a direct relationship with cutting forces.

VI. BIBLIOGRAPHY

Armarego, E.J. and Brown, R.H. *The machining of metals.* Prentice Hall, Englewood Cliffs, 1969.

Ataman, E., Aatre, V.K. and Wrong, K.M. "A fast method for real-time median filtering." *IEEE Trans.* ASSP-28, 1980.

Clarke, L.N. *A new dynamometer for measuring cutting forces in three dimensions.* Division of Forest Products, CSIRO, Melbourne, Australia, 1963.

Coombs, M. *Predicting the machinability of finger-joints in ponderosa pine cutting stock.* Unpublished Master's thesis, Oregon State University, 1988.

Dean, M. *Semiconductor and conventional strain gages.* Academic Press, 1962.

Dean, W. *Terms of the trade — a reference for the forest products industry.* Random Lengths Publications, 1978.

Franz, N.C. *An analysis of the wood-cutting process.* The University of Michigan Press, 1958.

Jones, C.W. "Fingerjointing can raise solid-wood recovery." *Forest Industries,* 117(6): 32-5, July/August 1990.

Klamecki, B.E. "Discontinuous chip formation in woodcutting—a catastrophe theory description." *Wood Science,* 12(1): 32-7, 1979.

Koch, P. *Wood machining processes.* The Ronald Press Company, 1964.

Loewen, E.G., Marshall, E.R., Shaw, M.C. "Electric strain gauge tool dynamometers." *Proceedings of the Society for Experimental Stress Analysis,* 8(2): 1-16, 1951.

McKenzie, W.M. "Basic aspects of inclined or oblique wood cutting." *Forest Products Journal,* 14(12): 555-66, 1964.

McKenzie, W.M. "Fundamental aspects of the wood cutting process." *Forest Products Journal,* 10(9): 447-56, 1960.

McKenzie, W.M. "The relationship between the cutting properties of wood and its physical and mechanical properties." *Forest Products Journal,* 12(6): 287-94, 1962.

McKenzie, W.M. and Hawkins, B.T. "Quality of near longitudinal wood Surfaces formed by inclined cutting." *Forest Products Journal*, 16(7): 35-8, 1966.

Perry, C.C. and Lissner, H.R. *The strain gage primer.* McGraw-Hill Book Co., New York, 1955.

Stewart, H.A. "Analysis of orthogonal woodcutting across the grain." *Wood Science*, 12(1): 38-45, July 1979.

Stewart, H.A. "Chip formation when orthogonally cutting wood against the grain." *Wood Science*, 3(4): 193-203, April 1971.

Stewart, H.A. "Effect of cutting direction with respect to grain angle on the quality of machined surface, tool force components, and cutting friction coefficient." *Forest Products Journal*, 19(3): 43-6, 1969.

Thomson, W.T. *Theory of vibration with applications,* 3rd ed. Prentice Hall, Englewood Cliffs, 1988.

Thompson, A.M. "A bridge for the measurement of permittivity." *Proc. Instn. Elect. Engrs.* B 103(12): 704-9, 1956.

Tuppeny, Jr., W.H. and Kobayashi, A.S. *Manual on experimental stress analysis.* Society for Experimental Stress Analysis, Westport, 1965.

Woodson, G.E. and Koch, P. *Tool forces and chip formation in orthogonal cutting of loblolly pine.* U.S.D.A. Forest Service Research Paper SO-52, 1970.